

# Histone Deacetylase HDAC8 Promotes Insulin Resistance and $\beta$ -Catenin Activation in NAFLD-Associated Hepatocellular Carcinoma

Yuan Tian<sup>1,2</sup>, Vincent W.S. Wong<sup>1,2</sup>, Grace L.H. Wong<sup>1,2</sup>, Weiqin Yang<sup>1,2</sup>, Hanyong Sun<sup>1,2</sup>, Jiayun Shen<sup>1,2</sup>, Joanna H.M. Tong<sup>3</sup>, Minnie Y.Y. Go<sup>1</sup>, Yue S. Cheung<sup>4</sup>, Paul B.S. Lai<sup>4</sup>, Mingyan Zhou<sup>1</sup>, Gang Xu<sup>1</sup>, Tim H.M. Huang<sup>5</sup>, Jun Yu<sup>1,2</sup>, Ka F. To<sup>2,3</sup>, Alfred S.L. Cheng<sup>2,6</sup>, and Henry L.Y. Chan<sup>1,2</sup>

## Abstract

The growing epidemic of obesity, which causes nonalcoholic fatty liver disease (NAFLD) and the more severe phenotype nonalcoholic steatohepatitis (NASH), has paralleled the increasing incidence of hepatocellular carcinoma (HCC). Accumulating evidence demonstrates that overnutrition and metabolic pathways can trigger modifications of DNA and histones via deregulation of chromatin modifiers, resulting in aberrant transcriptional activity. However, the epigenetic regulation of HCC development in NAFLD remains obscure. Here, we uncover key epigenetic regulators using both dietary and genetic obesity-promoted HCC models through quantitative expression profiling and characterize the oncogenic activities of histone deacetylase HDAC8 in NAFLD-associated hepatocarcinogenesis. HDAC8 is directly upregulated by the lipogenic transcription factor SREBP-1 where they are coexpressed in dietary obesity

models of NASH and HCC. Lentiviral-mediated HDAC8 attenuation *in vivo* reversed insulin resistance and reduced NAFLD-associated tumorigenicity. HDAC8 modulation by genetic and pharmacologic approaches inhibited p53/p21-mediated apoptosis and G<sub>2</sub>-M phase cell-cycle arrest and stimulated  $\beta$ -catenin-dependent cell proliferation. Mechanistically, HDAC8 physically interacted with the chromatin modifier EZH2 to concordantly repress Wnt antagonists via histone H4 deacetylation and H3 lysine 27 trimethylation. In human NAFLD-associated HCC, levels of SREBP-1, HDAC8, EZH2, H4 deacetylation, H3K27me3, and active  $\beta$ -catenin were all correlated positively in tumors compared with nontumor tissues. Overall, our findings show how HDAC8 drives NAFLD-associated hepatocarcinogenesis, offering a novel epigenetic target to prevent or treat HCC in obese patients. *Cancer Res*; 75(22); 4803–16. ©2015 AACR.

## Introduction

Recent large-scale prospective and population-based studies have pointed out that obesity was associated with increased incidence and mortality of several cancers (1, 2). Although the actual increase in risk varies among different cancer types, hepatocellular carcinoma (HCC) is one of the most severely affected

cancers in obese individuals (1–3). Obesity-induced hepatosteatosis, together with its more severe complication nonalcoholic steatohepatitis (NASH) classified as nonalcoholic fatty liver disease (NAFLD), can progress to cirrhosis, end-stage liver disease, or HCC (4–6). HCC is currently the fifth most common cancer and the third most common cause of cancer-related deaths worldwide. Given the prevalence of obesity in the developed countries and its rapid increase in developing countries (7), HCC arising from NAFLD will lead to further aggravation of this major global health problem.

Although recent next-generation sequencing studies have uncovered the genomic landscape of HCC (8, 9), the increasing incidence of HCC cannot be solely explained by the HCC genome. Emerging evidence demonstrates that overnutrition and metabolic pathways can trigger epigenetic modifications via deregulation of chromatin modifiers, leading to aberrant transcriptional activity during carcinogenesis (10–12). NAFLD is the hepatic manifestation of obesity and metabolic syndrome. The major hallmark of metabolic syndrome is insulin resistance, which is closely linked to HCC development (5, 6). Although altered DNA methylation may contribute to the progression of NAFLD (13, 14), the role of histone modifications in NAFLD-associated hepatocarcinogenesis has not yet been explored.

In this study, we identified histone deacetylase 8 (HDAC8) as a novel epigenetic modifier from 2 obesity-promoted HCC

<sup>1</sup>Department of Medicine and Therapeutics and Institute of Digestive Disease, The Chinese University of Hong Kong, Hong Kong SAR, PR China. <sup>2</sup>State Key Laboratory of Digestive Disease, The Chinese University of Hong Kong, Hong Kong SAR, PR China. <sup>3</sup>Department of Anatomical and Cellular Pathology, The Chinese University of Hong Kong, Hong Kong SAR, PR China. <sup>4</sup>Department of Surgery, The Chinese University of Hong Kong, Hong Kong SAR, PR China. <sup>5</sup>Department of Molecular Medicine, The University of Texas Health Science Center at San Antonio, San Antonio, Texas. <sup>6</sup>School of Biomedical Sciences, The Chinese University of Hong Kong, Hong Kong SAR, PR China.

**Corresponding Authors:** Alfred S.L. Cheng, The Chinese University of Hong Kong, Room 405, Lo Kwee-Seong Integrated Biomedical Sciences Building in Area 39, Hong Kong SAR, PR China. Phone: 852-3943-9842; Fax: 852-2603-5139; E-mail: alfredcheng@cuhk.edu.hk or Henry L.Y. Chan, Department of Medicine and Therapeutics, 9/F, Prince of Wales Hospital, Shatin, NT, Hong Kong SAR, PR China. Phone: 852-2632-3593; Fax: 852-2637-3852; E-mail: hlychan@cuhk.edu.hk

doi: 10.1158/0008-5472.CAN-14-3786

©2015 American Association for Cancer Research.

models and further characterized its effects on insulin resistance and aberrant proliferation via interaction with the polycomb protein enhancer of zeste homolog 2 (EZH2). These findings demonstrate the functional significance of HDAC8 in NAFLD-associated hepatocarcinogenesis, providing a strong impetus for therapeutic intervention via targeting specific chromatin regulators.

## Materials and Methods

### Cell culture, transfection, expression, and functional analysis

LO2, HepG2, Bel-7404, and PLC5 cells were cultured in DMEM supplemented with 10% FBS (Hyclone). Cell transfection was conducted using X-tremeGene Transfection Reagent (Roche) or HiPerfect (Qiagen) according to the manufacturer's instructions. The information of small-interfering RNA (siRNA), short-hairpin RNA (shRNA) constructs, and expression vectors is described in Supplementary Information. The methods for chromatin immunoprecipitation (ChIP), reverse transcription (RT)-PCR, Western blot, coimmunoprecipitation, luciferase reporter array, immunostaining, colony formation, MTS assay, and flow cytometry are also stated.

### Lentiviral-mediated shRNA knockdown in obesity-promoted NASH and HCC mouse models

The obesity-promoted HCC models were constructed as described previously with slight modification (Supplementary Fig. S1A; ref. 15). For the genetic obesity-HCC model, 14-day-old leptin receptor-deficient (db/db) mice on a C57BL/6 background and the corresponding age-matched heterozygous (db/m) lean control mice were intraperitoneally injected with 5 mg/kg diethylnitrosamine (DEN). All mice were maintained on autoclaved regular chow diet. For the dietary obesity-HCC model, DEN-treated C57BL/6 mice (6-week-old) were separated into two dietary groups and fed either low-fat diet (LFD, composed of 12% fat, 23% protein, 65% carbohydrates based on caloric content) or high-fat diet (HFD, composed of 60% fat, 15% protein, 25% carbohydrates based on caloric content; BioServ). For the dietary obesity-NASH model, 6-week-old male C57BL/6 mice were randomly assigned to LFD or high-fat, high-carbohydrate (HFHC) diet (Surwit diet) and drinking water enriched with high-fructose corn syrup equivalent as described previously (16). Lentiviruses encoding shRNA against *Hdac8* (shHdac8) or control sequence (shCtrl) were packaged according to the manufacturer's instructions (Dharmacon) for transduction in the dietary obesity models. At the age of 6 and 18 weeks,  $5 \times 10^7$  transducing units of lentiviruses in 100  $\mu$ L PBS were administered via tail vein injection as previously described (17, 18). Intraperitoneal glucose or insulin tolerance test (IPGTT/IPITT) was performed at the age of 26 weeks. All mice were sacrificed when 28 weeks old, and liver and blood samples were collected for expression analysis and metabolic profiling. Detailed description of the xenograft and orthotopic models (19) is provided in Supplementary Information. All animal studies were approved by the Chinese University of Hong Kong (CUHK) Animal Experimentation Ethics Committee.

### Quantitative expression profiling

Total RNAs extracted from 8 pairs of tumor and adjacent nontumor tissues of obese mice (HFD-fed or db/db, two pairs

each) and the lean controls (LFD-fed or db/m, two pairs each) were used for expression profiling of 115 chromatin regulators (listed in Supplementary Table S1) by customized RT<sup>2</sup> Profiler PCR Arrays (Qiagen). Histologic examination indicated that the proportion of HCCs in the tumor sections was 70% to 90% (Supplementary Fig. S1B). Quantitative RT-PCR validation was performed using additional tumor and nontumor tissues from HFD-fed (6 pairs) and db/db (7 pairs) obese mice and normal liver tissues from LFD-fed ( $n = 3$ ) and db/m ( $n = 7$ ) lean mice. The significant differentially expressed gene in tumors compared with nontumor and normal liver tissues was then verified by Western blot analysis.

### Patients and clinical specimens

Patients who underwent hepatectomy for NAFLD-associated HCC at the Prince of Wales Hospital (Hong Kong) were included in this study. All patients had history of metabolic syndrome, including diabetes, hypertension or dyslipidemia, and/or exhibited fatty liver changes. HCC patients with chronic hepatitis B and C, or record of alcoholic intake, have been excluded. All HCC patients gave written informed consent on the use of clinical specimens for research purposes. Studies using human tissue were approved by the Joint CUHK-NTEC Clinical Research Ethics Committee (CRE Ref. No. 2014.511).

### Statistical analysis

Statistical tests for data analysis included two-tailed Student *t*, Pearson *r*, Mann-Whitney's *U*, and  $\chi^2$  tests. A *P* value of  $<0.05$  was considered statistically significant.

## Results

### Upregulation of HDAC8 in murine NAFLD-associated HCC models

To investigate the epigenetic regulation of HCC development in NAFLD, we performed quantitative expression profiling of 115 chromatin regulators in 16 tumor and adjacent nontumor tissues from both dietary and genetic obesity-promoted HCC models (Fig. 1A). The HFD-induced or the homozygous leptin receptor-deficient (db/db) obese mice and the corresponding LFD or heterozygous (db/m) lean controls exposed to low-dose DEN were sacrificed at the age of 7 months (Supplementary Fig. S1A) as previously described (15). All dietary and genetic obese mice developed HCCs in NAFLD characterized by histologic features of steatohepatitis and hepatocellular ballooning (Supplementary Fig. S1B) and activation of inflammatory signaling pathways (Supplementary Fig. S1C–S1F). Fifty and 12 differentially expressed genes (defined as 2-fold difference) were uncovered in dietary and genetic obesity-promoted tumors compared with nontumor tissues, respectively (Supplementary Table S1), of which four genes (*Cbx3*, *Cbx7*, *Hdac8*, and *Suz12*) were commonly deregulated in both models (Fig. 1A). Using additional normal liver, nontumor, and tumor tissues from dietary ( $n = 15$ ) and genetic ( $n = 21$ ) obesity models, *Hdac8* was identified as the sole significantly upregulated chromatin regulator in obesity-promoted HCCs by quantitative RT-PCR ( $P < 0.001$  and  $0.01$ ; Fig. 1B) and further confirmed by Western blot analysis (Fig. 1C). Immunohistochemistry demonstrated that *Hdac8* protein was highly expressed in the nuclei of tumor cells in both HCC models (Fig. 1D). Consistently, immunofluorescence showed nuclear HDAC8 staining in human BEL-

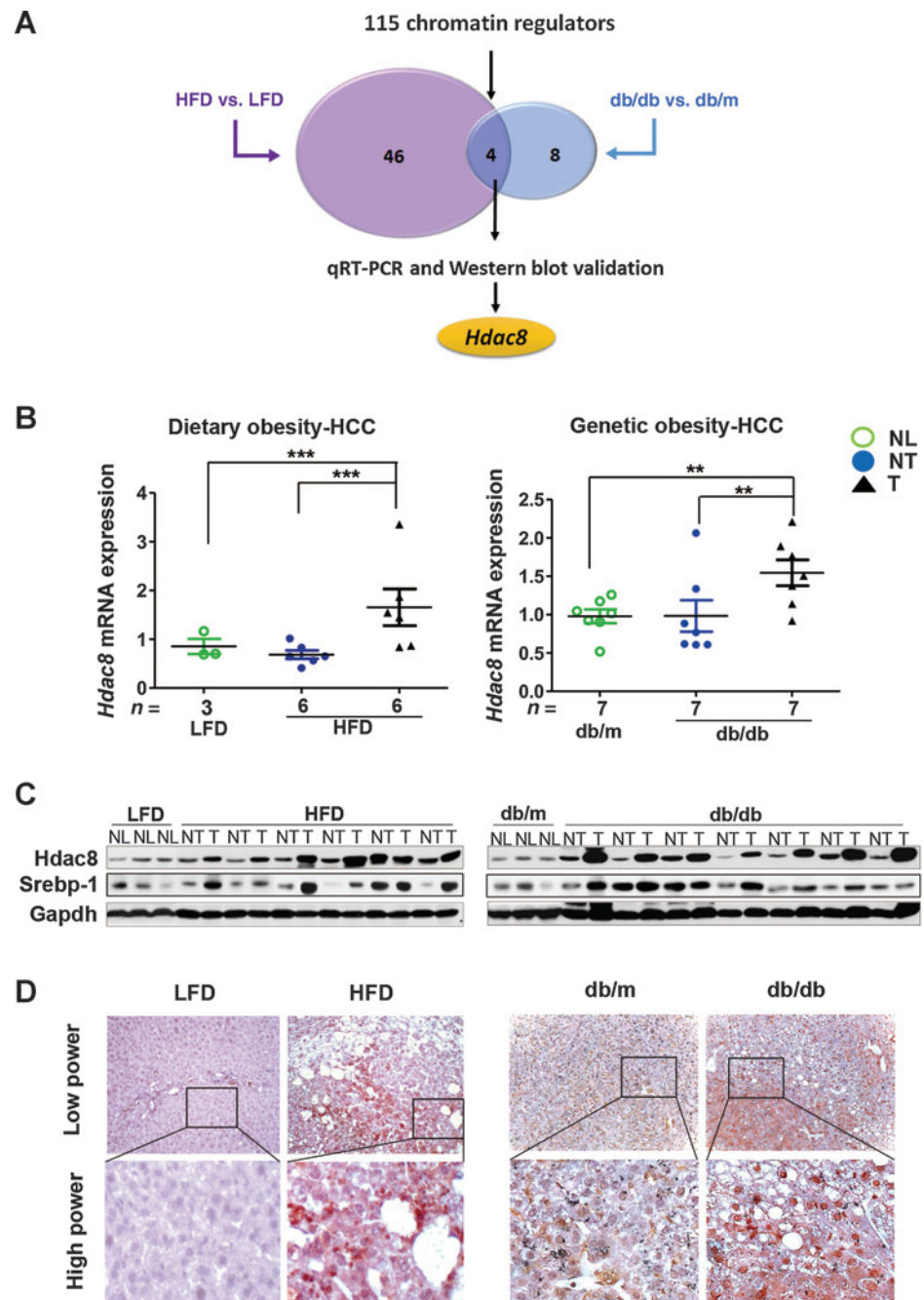


**Figure 1.** Upregulation of Hdac8 in murine NAFLD-associated HCC models. A, overview of the targeted gene profiling approach to nominate critical epigenetic modifier for detailed analysis. B and C, qRT-PCR (B) and Western blot (C) validation of Hdac8 overexpression in NAFLD-associated HCC models (NL, normal livers; NT, adjacent nontumors; T, tumors; \*\*,  $P < 0.01$ ; \*\*\*,  $P < 0.001$ ). D, representative pictures of Hdac8 immunohistochemical staining in livers of control groups (LFD and db/m) and obesity groups (HFD and db/db). Low power magnification,  $\times 200$ ; high power magnification,  $\times 400$ .

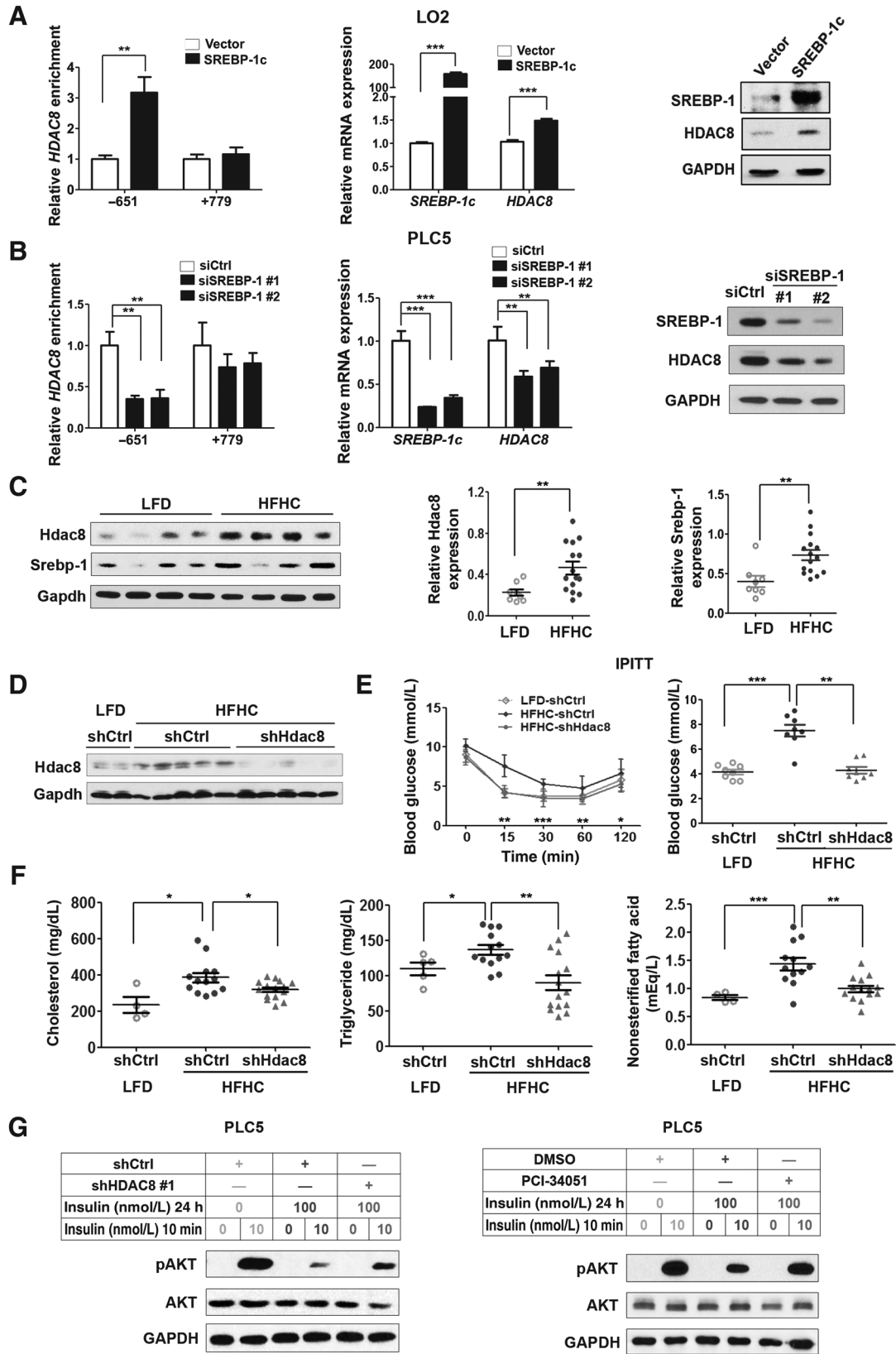
7404 and PLC5 HCC cells but not HepG2 hepatoblastoma cells and immortalized LO2 hepatocytes (Supplementary Fig. S2A). Moreover, Western blot demonstrated an inverse relationship between HDAC8 and histone H4 acetylation (H4ac) in cell lines (Supplementary Fig. S2B) and obesity-HCC models (Supplementary Fig. S1C and S1D).

**HDAC8 is directly upregulated by SREBP-1 and coexpressed in dietary obesity models of NASH and HCC**

To explore its transcriptional regulation in NAFLD-associated HCC, we performed HDAC8 promoter analysis using the TRANS-

FAC database and identified two putative binding sites of sterol regulatory element-binding protein-1 (SREBP-1), a master regulator of *de novo* lipogenesis contributing to NAFLD progression (Supplementary Fig. S2C; refs. 20, 21). Ectopic expression of SREBP-1c in both low HDAC8-expressing LO2 and HepG2 cells (Supplementary Fig. S2D) increased its occupancy at the sterol regulatory element (SRE) upstream (-651 bp) but not downstream (+779 bp) of the HDAC8 transcription start site (Fig. 2A, left; Supplementary Fig. S2E) in consistent with the higher similarity scores from the TRANSFAC database (Supplementary Fig. S2C). Moreover, the mRNA and protein expressions of HDAC8

Downloaded from <http://aacrjournals.org/cancerres/article-pdf/75/22/4803/2937406/4803.pdf> by guest on 18 March 2025





were also increased (Fig. 2A middle, right; Supplementary Fig. S2E). Conversely, siRNA-mediated knockdown of SREBP-1 in both HDAC8-expressing PLC5 and BEL-7404 cells reduced the upstream SRE occupancy by SREBP-1 and HDAC8 gene expression levels (Fig. 2B; Supplementary Fig. S2F). These data demonstrate that SREBP-1 directly upregulates HDAC8 expression via promoter occupancy.

We next examined the pathophysiologic relevance of this finding using a murine model of obesity, insulin resistance, and NASH caused by diet high in saturated fat and fructose (Supplementary Fig. S3A; ref. 16). Western blot demonstrated significantly higher protein expressions of Hdac8 and Srebp-1 in HFHC-induced NASH compared with normal liver tissues of the LFD control group ( $P < 0.01$ ; Fig. 2C). Consistent with Srebp-1, its downstream lipogenic gene expressions were found to be increased in HFHC-induced NASH (Supplementary Fig. S3B). Moreover, concordant upregulation of Hdac8, Srebp-1, and lipogenic genes was also observed in the obesity-promoted HCC tissues (Fig. 1C; Supplementary Fig. S1E and S1F). Collectively, these *in vitro* and *in vivo* data support the notion that Hdac8 can be upregulated by the lipogenic transcription factor in NAFLD-associated hepatocarcinogenesis.

#### HDAC8 promotes insulin resistance *in vivo* and *in vitro*

Because SREBP-1 has been demonstrated to elicit insulin resistance crucial for HCC development (22, 23), we next investigated whether HDAC8 regulates insulin sensitivity using genetic modulation in the dietary obesity-NASH model. Administration of lentivirus expressing shHdac8 significantly reduced Hdac8 but not the other Class I Hdac isoforms expression in livers of the obese mice compared with those treated with shCtrl ( $P < 0.05$ ; Fig. 2D; Supplementary Fig. S3C) and reversed the insulin resistance as measured by IPITT ( $P < 0.05$ ; Fig. 2E). Moreover, Hdac8 knockdown nearly restored the plasma cholesterol, triglyceride, and nonessential fatty acid (NEFA) concentrations to the basal levels ( $P < 0.05$ ; Fig. 2F). The improved metabolic profile was also accompanied by reduced hepatocellular ballooning and inflammatory cell infiltration (Supplementary Fig. S3D).

We further examined whether HDAC8 promotes insulin resistance using an established cell model (24). HDAC8-expressing PLC5 cells transduced by lentivirus expressing shCtrl were preincubated for 24 hours with or without 100 nmol/L insulin, after which cells were treated acutely for 10 minutes with or without 10 nmol/L insulin (Supplementary Fig. S3E). High-dose insulin before incubation impaired the insulin sensitivity of PLC5 cells evident by dramatic reduction in phosphorylation of AKT at Ser473 (pAKT) upon acute insulin stimulation (Fig. 2G, left; ref. 24). The decreased pAKT level was accompanied by the abrogation of insulin-stimulated upregulation of lipogenic genes, namely fatty acid synthase (FAS) and liver X

receptor  $\alpha$  (*LXR $\alpha$* ; Supplementary Fig. S3F). Notably, in the insulin-resistant condition, PLC5 cells transduced by lentiviruses expressing two independent shHDAC8 showed enhancement of insulin-stimulated pAKT (Fig. 2G, left; Supplementary Fig. S3G) and lipogenic gene expressions (Supplementary Fig. S3F). To validate these findings, we used a pharmacologic approach using a potent inhibitor, PCI-34051 (25), which showed specific inhibition against HDAC8 but not the other class I HDAC isoforms (Supplementary Fig. S3H). Consistently, PCI-34051 treatment in PLC5 cells rescued insulin sensitivity as demonstrated by significant increase in pAKT (Fig. 2G, right) and lipogenic gene transcript levels (Supplementary Fig. S3F). Taken together, our findings suggest that HDAC8 promotes insulin resistance in both animal and cell models.

#### Downregulation of HDAC8 inhibits NAFLD-HCC tumorigenicity *in vivo*

To investigate whether HDAC8 induces NAFLD-associated hepatocarcinogenesis, we performed lentiviral-mediated knockdown of Hdac8 in the dietary obesity-HCC model (Supplementary Fig. S4A). Notably, downregulation of Hdac8 in livers of the obese mice ( $P < 0.001$ ; Fig. 3A) significantly reduced >60% NAFLD-associated tumor multiplicity and size ( $P < 0.05$ ; Fig. 3B; Supplementary Fig. S4B). The reduced tumorigenicity was associated with significant reduction in hepatocellular lipid accumulation as shown by Oil Red O staining ( $P < 0.05$ ; Fig. 3C). Consistently, the glucose sensitivity measured by IPGTT (Fig. 3D) and the plasma NEFA and triglyceride concentrations (Fig. 3E) were significantly restored to nearly the basal levels ( $P < 0.05$ ).

We further validated the oncogenicity of HDAC8 using both xenograft and orthotopic models. HDAC8 stably transfected LO2 or HepG2 cells and the corresponding empty vector-transfected cells were injected into the dorsal flanks of nude mice ( $n = 5$  per group) in the xenograft model. Both HDAC8-LO2 and HDAC8-HepG2 cells displayed remarkable tumor growth when compared with control cells ( $P < 0.001$  and  $P < 0.01$ ; Fig. 3F). In contrast, both shHDAC8-expressing BEL-7404 and PLC5 cells showed significantly reduced tumor growth when compared with cells expressing shCtrl ( $P < 0.05$  and  $P < 0.01$ ; Fig. 3G). In the orthotopic model, the tumors formed by the shHDAC8-BEL-7404 orthografts were significantly smaller when compared with the shCtrl orthografts ( $P < 0.05$ ; Fig. 3H). These results show that HDAC8 exhibits strong HCC oncogenicity *in vivo*.

#### HDAC8 promotes growth and inhibits apoptosis of HCC cells

To delineate the HDAC8 oncogenic activity, we first performed colony formation and cell proliferation assays upon genetic modulation and pharmacologic inhibition. Ectopic expression of HDAC8 in LO2 and HepG2 cells significantly induced

**Figure 2.**

HDAC8 promotes insulin resistance. A and B, ectopic expression (A) and knockdown (B) experiments demonstrated that SREBP-1 directly upregulates HDAC8 as shown by quantitative ChIP-PCR (left), RT-PCR (middle), and Western blot analysis (right). C, Western blot and semiquantitation of Hdac8 and Srebp-1 expressions in livers of the LFD- and HFHC-fed mice. D, Western blot of Hdac8 in livers of the LFD- and HFHC-fed mice following lentivirus administration. E, IPITT performed on LFD- and HFHC-fed mice at 26 weeks following lentivirus administration. Blood glucose was measured at indicated timepoints after insulin injection (left). Blood glucose levels at 15 minute are shown in the graph (right). F, plasma cholesterol, triglyceride, and NEFA levels of mice at 28 weeks. G, Western blot of pAKT and AKT expression in PLC5 cells stably transduced with shRNA-expressing lentivirus (left) or treated with 25  $\mu$ mol/L PCI-34051 (right).

\*,  $P < 0.05$ ; \*\*,  $P < 0.01$ ; \*\*\*,  $P < 0.001$ .

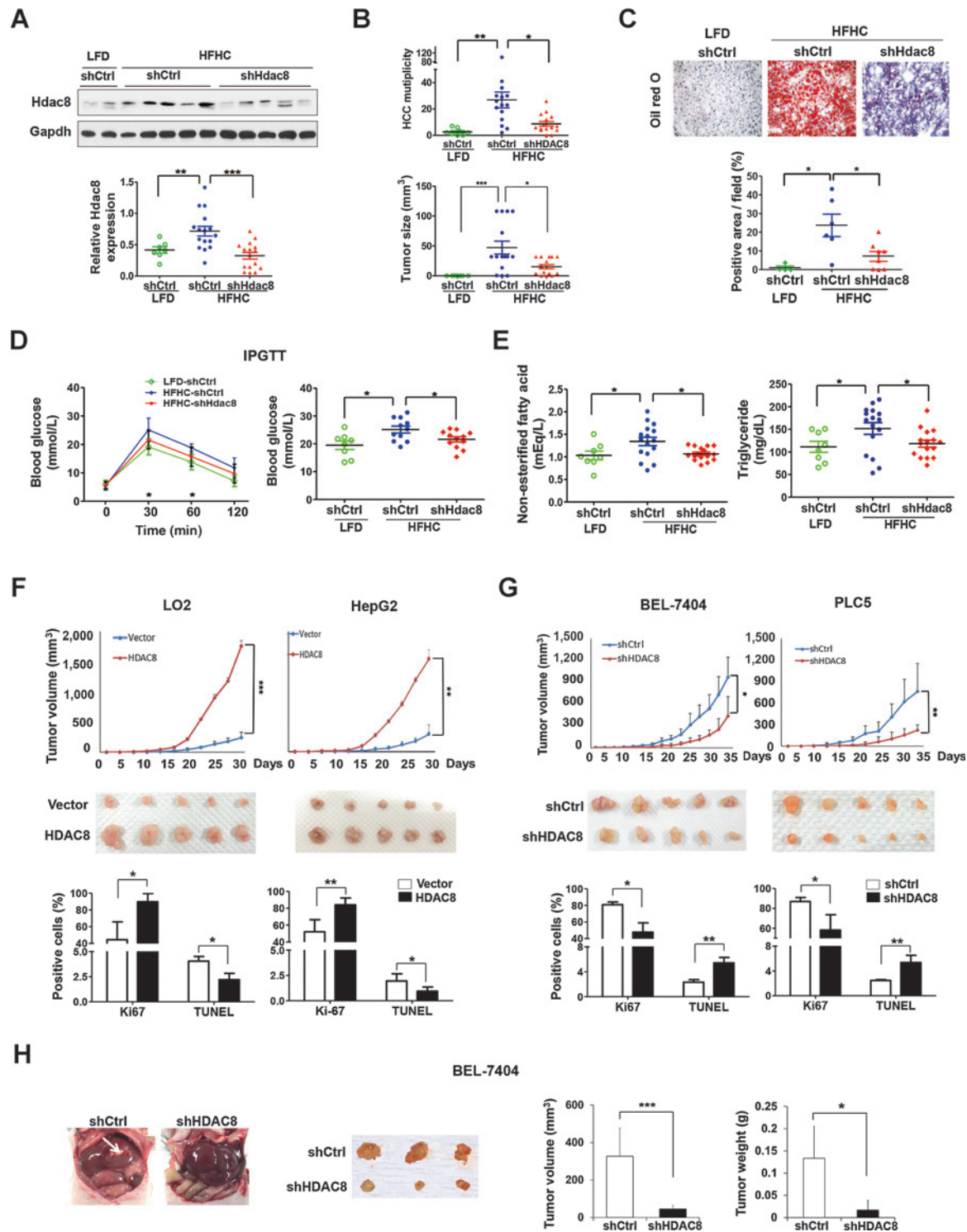


**Figure 3.** Downregulation of HDAC8 inhibits NAFLD-HCC tumorigenicity *in vivo*. A, Western blot and semiquantitation of Hdac8 expression in livers of the DEN-treated, LFD-, or HFD-fed mice administered with lentivirus expressing shCtrl or shHdac8. B and C, the averaged tumor multiplicity and size (B) and Oil Red O staining (C) in livers of the LFD- and HFD-fed mice following lentivirus administration. The percentages of positively-stained areas are shown in the graph. D, IPGTT performed on the three groups of mice at 26 weeks. Blood glucose was measured at indicated timepoints after glucose injection (left). Blood glucose levels at 30 minute are shown in the graph (right). E, plasma NEFA and triglyceride levels of mice at 28 weeks. F, tumor volume and images of xenografts derived from vector control or HDAC8 overexpressing LO2 and HepG2 cells. The quantitation of Ki-67 and TUNEL staining of nodules formed by the vector control and HDAC8 groups ( $n = 5$ ) is shown in the graph. G, tumor volume and images of xenografts derived from control shCtrl- and shHDAC8-BEL-7404 or PLC5 HCC cells. The quantitation of Ki-67 and TUNEL staining in both groups ( $n = 5$ ) is shown in the graph. H, representative tumor images, volume, and weight of the orthotopic model derived from shCtrl- and shHDAC8-BEL-7404 HCC cells ( $n = 3$ ). Original magnification,  $\times 200$ ; \*,  $P < 0.05$ ; \*\*,  $P < 0.01$ ; \*\*\*,  $P < 0.001$ .

cellular proliferation ( $P < 0.01$  and  $P < 0.05$ ), whereas lentiviral-mediated knockdown of HDAC8 in BEL-7404 and PLC5 HCC cells resulted in marked growth inhibition ( $P < 0.01$ ; Fig. 4A; Supplementary Fig. S5A and S5B). Consistently, PCI-34051 treatment caused a dose- and time-dependent inhibition of BEL-7404 and PLC5 cell proliferation ( $P < 0.01$ ; Fig. 4B). However, only minimal effect was observed in low HDAC8-expressing LO2 and HepG2 cells (Fig. 4B), thus validating the selectivity of PCI-34051 action. HDAC8 overexpression in LO2 and HepG2 cells decreased the levels of H4ac and p53, which was associated with reduction of apoptosis evident by cleaved PARP expression and Annexin V staining ( $P < 0.05$ ; Fig. 4C, left; Supplementary Fig. S5C). Conversely, knockdown of HDAC8 by two independent siRNAs in BEL-7404 and PLC5 cells increased the expression levels of H4ac, p53, and cleaved PARP accompanied by significant induction of apoptosis ( $P < 0.01$ ; Fig. 4C, right; Supplementary Fig. S5C). Consistently, PCI-34051 dose-dependently increased the expression levels of H4ac, p53, cleaved PARP, and the apoptotic populations in both BEL-7404 and PLC5 cells ( $P < 0.01$ ; Fig. 4D).

In addition, overexpression and knockdown of HDAC8 significantly reduced and increased the fractions of cells in G<sub>2</sub>-M phase, respectively ( $P < 0.05$  and  $P < 0.01$ ; Fig. 4E; Supplementary Fig. S5D). However, no consistent effect was observed in G<sub>1</sub> phase and S phase. Moreover, PCI-34051 decreased and increased the fractions of cells in G<sub>1</sub> phase and G<sub>2</sub>-M phase, respectively, in a dose-dependent manner ( $P < 0.001$ ; Fig. 4F). Together with the concomitant suppression of p21 by HDAC8 (Fig. 4C and D; Supplementary Fig. S5C), these data suggest that HDAC8 prohibits p21-dependent G<sub>2</sub>-M-phase arrest (26, 27).

Consistent with these *in vitro* data, HDAC8-LO2 and HDAC8-HepG2 tumor nodules showed significantly more proliferating cells and less apoptotic cells as assessed by Ki-67 and TUNEL staining, respectively ( $P < 0.05$ ; Fig. 3F; Supplementary Fig. S4C). Conversely, HCC growth inhibition by HDAC8 knockdown in BEL-7404 and PLC5 cells was accompanied by significant reduction in tumor cell proliferation ( $P < 0.05$ ) and induction of apoptosis ( $P < 0.01$ ; Fig. 3G; Supplementary Fig. S4D). Overall, these findings demonstrate the growth-promoting effect of HDAC8 via inhibition of apoptosis and cell-cycle arrest.

#### HDAC8 activates $\beta$ -catenin signaling to promote hepatocellular growth

To elucidate the mechanism underlying HDAC8-induced hepatocarcinogenesis, we determined the effect of HDAC8 on 10 cancer-related transcription factor activities using a luciferase reporter array. Ectopic HDAC8 expression in LO2 cells significantly and reproducibly increased the  $\beta$ -catenin/TCF and E2F, but diminished SMAD2/3/4 transcriptional activity ( $P < 0.05$ ; Fig. 5A; Supplementary Fig. S6A). Consistent with the suppression of p53 expression by HDAC8 (Fig. 4C and D; Supplementary Fig. S5C), the p53 transcriptional activity was also significantly inhibited ( $P < 0.05$ ). Because  $\beta$ -catenin/TCF has the highest activity and the importance of this signaling in hepatocarcinogenesis (28), its regulation by HDAC8 was further characterized. Concordant with the luciferase activity data, HDAC8 increased the expressions of active (dephosphorylated)  $\beta$ -catenin and its downstream pro-proliferative target cyclin D1 (CCND1) in both transcript ( $P < 0.01$ ) and protein levels

(Fig. 5B). On the contrary, inhibition of HDAC8 by either siRNAs or PCI-34051 in PLC5 and BEL-7404 cells reduced active  $\beta$ -catenin and CCND1 expressions (Fig. 5C and D; Supplementary Fig. S6B and S6C). To investigate the effect of  $\beta$ -catenin signaling on HDAC8-induced cell growth, colony formation assay was performed on LO2 and HepG2 cells cotransfected with vectors expressing HDAC8 and sh $\beta$ -catenin. Notably, downregulation of  $\beta$ -catenin in HDAC8-expressing cells significantly abrogated HDAC8-induced  $\beta$ -catenin activity (Fig. 5E; Supplementary Fig. S6D) and colony formation (Fig. 5F; Supplementary Fig. S6E). These results suggest that HDAC8 promotes proliferation through  $\beta$ -catenin activation in liver and HCC cells.

#### HDAC8 acts in concert with EZH2 to epigenetically repress Wnt antagonists

To further unravel the molecular pathway by which HDAC8 activates  $\beta$ -catenin signaling, we examined the epigenetic regulation of Wnt antagonists by HDAC8. Ectopic HDAC8 expression in LO2 and HepG2 cells significantly reduced the expressions of the EZH2-bound Wnt antagonists (29), namely, *AXIN2*, *NKD1*, *PPP2R2B*, and *PRICKLE1* ( $P < 0.01$  and  $P < 0.05$ ; Fig. 6A; Supplementary Fig. S7A). Conversely, inhibition of HDAC8 in BEL-7404 cells using two independent siRNAs or PCI-34051 led to concordant upregulation of the Wnt antagonists (Fig. 6B). Consistent results were also observed in PLC5 cells (Supplementary Fig. S7B). We next determined whether HDAC8 epigenetically represses Wnt antagonist expressions. By combining quantitative ChIP-PCR with RNA interference, we found that knockdown of HDAC8 by two independent siRNAs not only decreased the promoter occupancy of its own, but also EZH2 in both BEL-7404 and PLC5 cells (Fig. 6C; Supplementary Fig. S7C). In agreement with the loss of these binding activities, H4ac and histone H3 lysine 27 trimethylation (H3K27me3) modifications were increased and decreased, respectively (Fig. 6C; Supplementary Fig. S7C). To determine whether HDAC8 physically interacts with EZH2, we conducted coimmunoprecipitation and detected a robust physical interaction between HDAC8 and EZH2 in both BEL-7404 and PLC5 cells (Fig. 6D; Supplementary Fig. S7D). To demonstrate the promoter co-occupancy of HDAC8 and EZH2, pairwise sequential ChIP was carried out. After the EZH2 first ChIP, HDAC8 recruitment was enriched in EZH2-bound *AXIN2*, *NKD1*, and *PPP2R2B* promoters, but not in a negative control region (Fig. 6E, left), indicating that HDAC8 was concurrently enriched to these promoters with EZH2. Similar results were also obtained in HDAC8 first ChIP experiments (Fig. 6E, right).

To further investigate whether this regulatory pathway is perturbed *in vivo*, we examined the expressions of the chromatin regulators and signaling molecules in the dietary and genetic obesity-promoted HCC models. In accordance with *Hdac8* upregulation, *Ezh2*, H3K27me3, active  $\beta$ -catenin, and *Ccnd1* levels were significantly increased in tumors compared with adjacent liver tissues of both HFD-fed ( $P < 0.05$ ) and db/db mice ( $P < 0.05$ ; Fig. 6F and G; Supplementary Fig. S7E). Moreover, *Hdac8* downregulation markedly suppressed the *Ezh2*- $\beta$ -catenin cascade in livers of the dietary obesity-HCC model (Fig. 6H). Collectively, these data are in line with the *in vitro* findings that HDAC8 and EZH2 cooperatively repress Wnt antagonists via histone deacetylation and trimethylation.

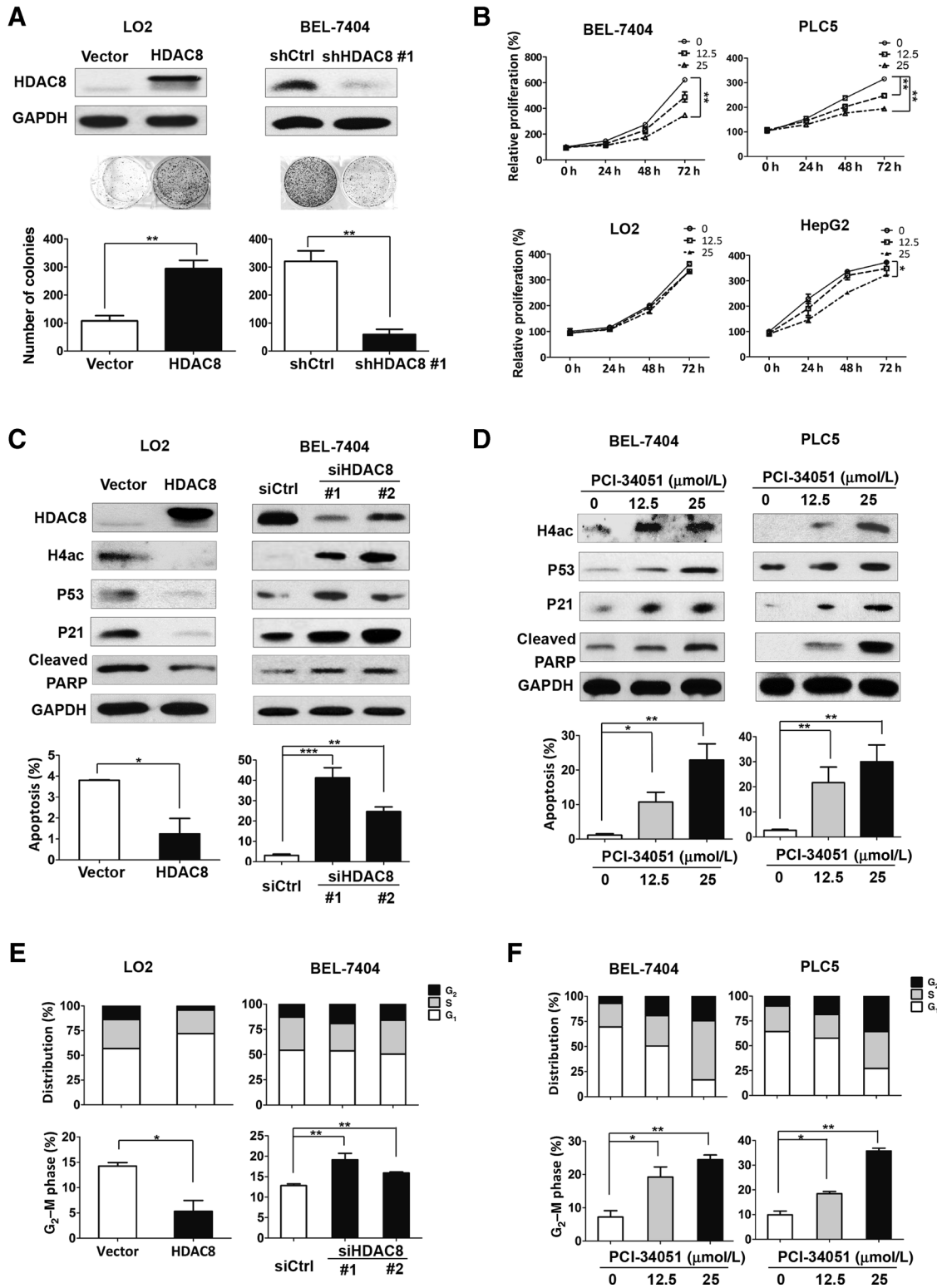


**Figure 4.** HDAC8 promotes growth and inhibits apoptosis of HCC cells. A, colony formation assay of vector control or HDAC8 overexpressing LO2 cells (left) and BEL-7404 cells stably transfected with lentivirus expressing shCtrl or shHDAC8 (right). B, MTS assays of liver and HCC cells treated with different doses (μmol/L) of HDAC8 inhibitor. C, Western blot of H4ac, p53, p21, and cleaved PARP expressions (top) and Annexin V staining of cell apoptosis (bottom) in control or HDAC8 overexpressing LO2 cells (left) and BEL-7404 cells transfected with siRNAs against control sequence or *HDAC8* (right). D, Western blot (top) and Annexin V staining (bottom) in BEL-7404 (left) and PLC5 (right) cells treated with PCI-34051. E and F, flow cytometry of cell-cycle distribution in control or HDAC8 overexpressing LO2 cells (left), BEL-7404 cells transfected with siRNAs against control sequence or *HDAC8* (right; E), and BEL-7404 (left) and PLC5 (right) cells treated with PCI-34051 (F). \*,  $P < 0.05$ ; \*\*,  $P < 0.01$ ; \*\*\*,  $P < 0.001$ .



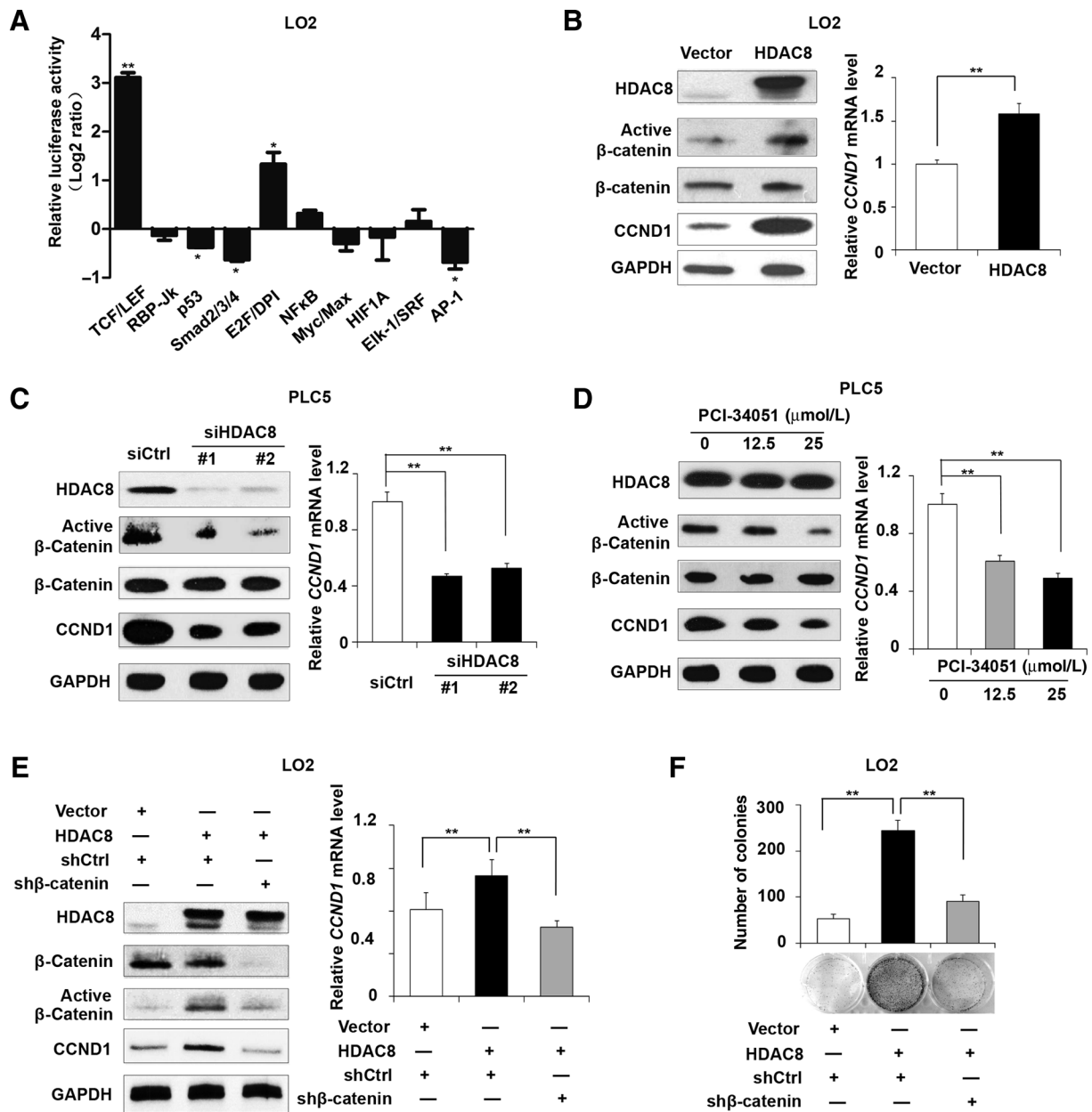


**Figure 5.** HDAC8 activates β-catenin signaling to promote hepatocellular growth. A, luciferase reporter array revealed signal deregulation by HDAC8 in overexpressing LO2 cells. B, ectopic expression of HDAC8-promoted Wnt/β-catenin signaling activity determined by Western blot (left) and qRT-PCR (right) analysis. C and D, knockdown (C) of HDAC8 and HDAC8 inhibitor (D)-suppressed Wnt/β-catenin signaling activity determined by Western blot (left) and qRT-PCR (right) analysis. E and F, knockdown of β-catenin abolished HDAC8-promoted Wnt/β-catenin signaling activity determined by (E) Western blot (left), quantitative RT-PCR (right), and (F) colony formation assay. \*,  $P < 0.05$ ; \*\*,  $P < 0.01$ .

**Significant correlations between HDAC8 and its signaling components in primary human NAFLD-associated HCCs**

To investigate the clinical relevance of our findings, the protein levels of SREBP-1, HDAC8, H4ac, EZH2, H3K27me3, pAKT, and active β-catenin were examined by Western blot in 24 pairs of human NAFLD-associated HCCs with neither viral nor alcoholic hepatitis (Supplementary Table S2). Compared with the paired nontumor liver tissues, significant upregulation of SREBP-1, HDAC8, EZH2, H3K27me3, and active β-catenin and downregu-

lation of H4ac and pAKT were detected in HCC tissues ( $P < 0.01$ ; Fig. 7A). Significant elevation of *SREBP-1c*, *HDAC8*, and *CCND1* transcript levels was also observed in the clinical specimens ( $P < 0.01$ ; Supplementary Fig. S8). Overall, the trends of protein expressions were concordant with the murine obesity-promoted HCC models (Figs. 1C and 6F and G; Supplementary Fig. S1C and S1D). Association analysis further showed positive correlations between SREBP-1 and HDAC8 ( $r = 0.4007$ ), HDAC8 and EZH2 ( $r = 0.3240$ ), EZH2 and H3K27me3 ( $r = 0.4254$ ),

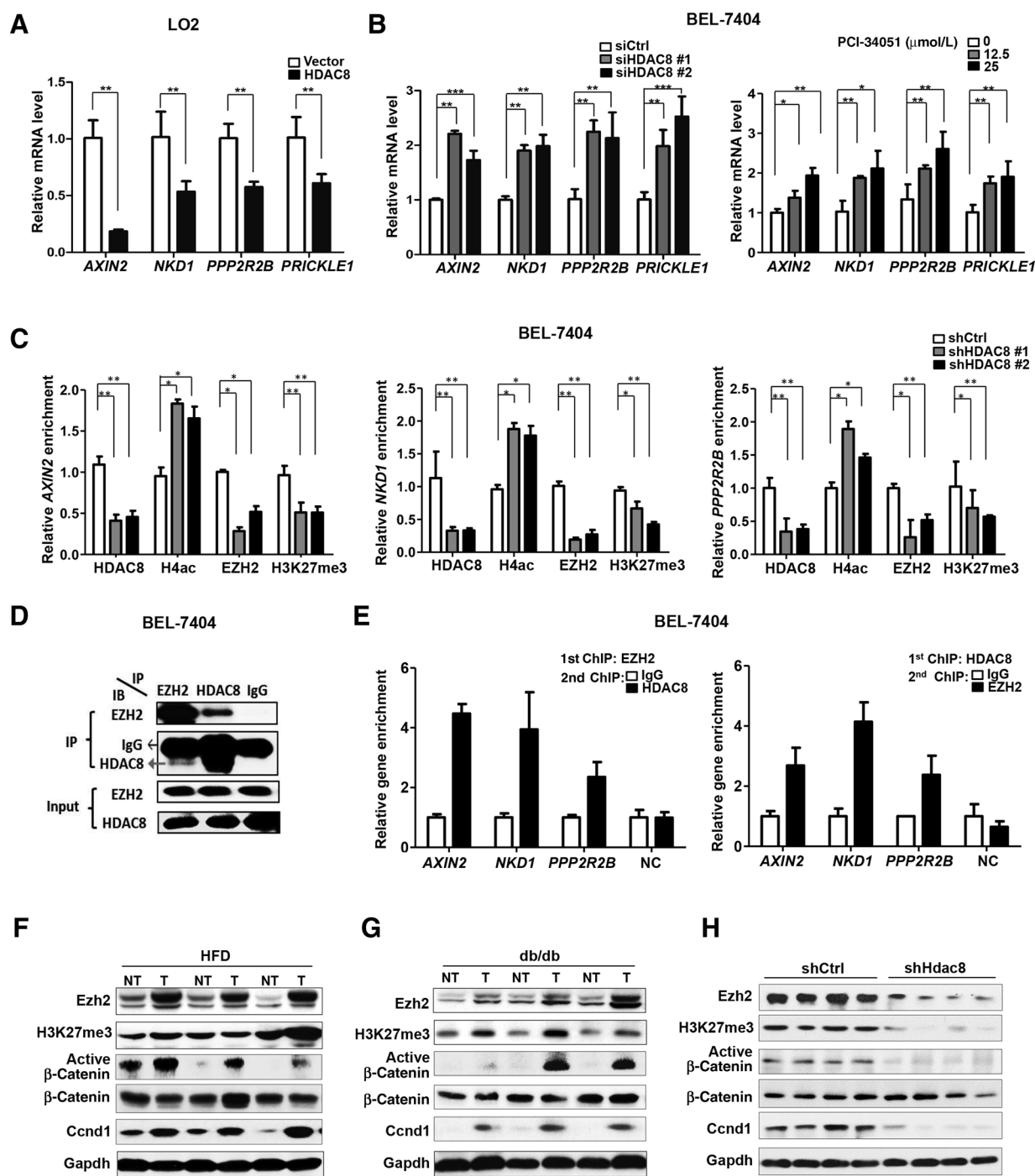


**Figure 6.**

HDAC8 acts in concert with EZH2 to epigenetically repress Wnt antagonists. A and B, qRT-PCR analysis of Wnt antagonists in LO2 cells following ectopic HDAC8 expression (A) and BEL-7404 cells upon HDAC8 siRNAs and PCI-34051 treatment (B). C, quantitative ChIP-PCR of HDAC8, EZH2 occupancy, and histone modifications in *AXIN2*, *NKD1*, and *PPP2R2B* promoters of BEL-7404 cells upon HDAC8 knockdown by two independent shRNA constructs. D, coimmunoprecipitation of HDAC8 and EZH2 in BEL-7404 cells. IgG represents a control antibody used for immunoprecipitates (IP). Total lysates were used as input controls. E, re-ChIP assay was performed to assess promoter co-occupancy of HDAC8 and EZH2 in BEL-7404 cells. First ChIP and second ChIP antibodies are indicated in the graph. Relative enrichment is represented as fold change to control IgG second ChIP. A nontarget region served as a negative control (NC). F and G, Western blot of Ezh2, H3K27me3, active  $\beta$ -catenin,  $\beta$ -catenin, and Ccnd1 proteins in representative tumors (T) and paired nontumors (NT) from dietary (F) and genetic (G) obesity-promoted HCC models. H, Western blot analysis of liver tissues of the DEN-treated and HFD-fed mice administered with lentivirus expressing shCtrl or shHdac8. \*,  $P < 0.05$ ; \*\*,  $P < 0.01$ ; \*\*\*,  $P < 0.001$ .

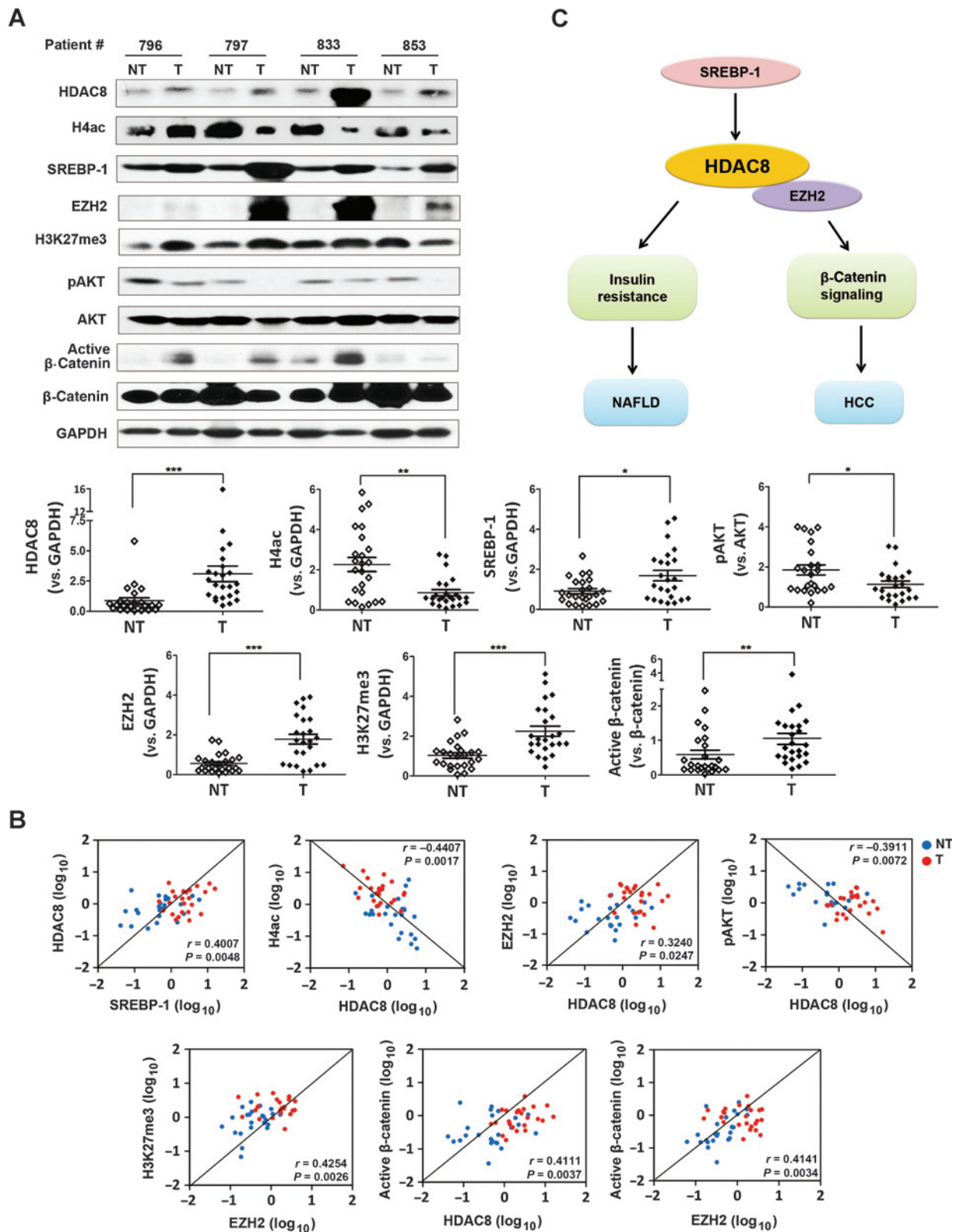


**Figure 7.** HDAC8 expression positively correlates with its signaling components in primary human NAFLD-associated HCCs. **A**, Western blot analysis of HDAC8, SREBP-1, EZH2, histone modifications, β-catenin signaling, and AKT phosphorylation in human NAFLD-associated HCC. Representative Western blot pictures (top) and relative protein expression levels (bottom) of tumors (T) and adjacent nontumors (NT) from 24 paired NAFLD-associated HCCs. **B**, correlations among SREBP-1, HDAC8, EZH2, H4ac, H3K27me3, pAKT, and active β-catenin in NAFLD-associated HCC patient samples. \*,  $P < 0.05$ ; \*\*,  $P < 0.01$ ; \*\*\*,  $P < 0.001$ . **C**, a working model of the deregulation and oncogenicity of HDAC8 in NAFLD-associated HCC.

HDAC8 and active  $\beta$ -catenin ( $r = 0.4111$ ), and EZH2 and active  $\beta$ -catenin ( $r = 0.4141$ ), and negative correlations between HDAC8 and H4ac ( $r = -0.4407$ ) and HDAC8 and pAKT ( $r = -0.3911$ ;  $P < 0.05$ ; Fig. 7B).

## Discussion

One of the most remarkable findings of the recent cancer genome sequencing studies is the repeated discovery of somatic driver mutations in genes that encode chromatin-remodeling factors (30). Characterization of the genomic landscape of HCC has revealed that as much as 50% of the primary tumors are estimated to harbor mutations in different chromatin regulators, providing strong evidence that epigenome disruption is a major hallmark of HCC (8, 9). In addition to somatic mutations, transcriptional deregulation also causes malfunction of chromatin regulators in cancer (31). In this study, we have identified HDAC8 as a pivotal chromatin regulator in the development of NAFLD-associated HCC through aberrant upregulation by the lipogenic transcription factor SREBP-1. We have elucidated previously unexplored functions of HDAC8 in promoting insulin resistance in NAFLD progression and  $\beta$ -catenin-dependent cell proliferation through interacting with another critical chromatin regulator EZH2 (Fig. 7C).

HDAC8 is the least characterized class 1 HDAC originally cloned in 2000 (32–34). Although HDAC1, 2, and 3 are active as subunits of multiprotein complexes, an HDAC8 complex has not been identified (35). HDAC8 expression is restricted to specific cell type showing smooth muscle differentiation in normal human tissues (34, 36). Although HDAC8 has been shown to promote growth of a number of cancer types (25), (37–39) and contribute to poor prognosis in childhood neuroblastoma (40), the molecular actions of HDAC8 in cancer remained poorly defined. Although specific HDACs can deacetylate nonhistone proteins (35), emerging data suggest that direct gene repression by HDAC8 might control key pathologic processes (41, 42). Kang and colleagues have recently found that HDAC8 transcriptionally represses *BMF*, a Bcl-2 protein family member, to interfere BMF-mediated apoptosis in colon cancer cells (42). Our present data demonstrate that HDAC8 acts in concert with EZH2 to epigenetically silence the Wnt antagonists *AXIN2*, *NKD1*, *PPP2R2B*, and *PRICKLE1*, leading to  $\beta$ -catenin activation and consequential cell proliferation. The control of H4 acetylation by the nuclear-predominant HDAC8 in cancer cells and their inverse correlation in murine and clinical specimens further support our conclusion that HDAC8 functions as an epigenetic regulator in HCC development. Consistent with the reports on p53 regulation by HDAC8 (39, 43), we found that HDAC8 inhibits the p53 transcriptional activity and p21 expression, which may contribute to the marked reduction in apoptosis and G<sub>2</sub>-M-phase arrest. The dramatic inhibition of xenograft and orthotopic tumor growth via induction of apoptosis by HDAC8 knockdown further establishes the strong oncogenic activity of HDAC8 in HCC.

Result from our luciferase reporter array indicates that HDAC8 modulates TGF $\beta$  and mitogen-activated protein kinase/c-Jun N-terminal kinase (MAPK/JNK) signaling reported to contribute to hepatic steatosis, insulin resistance, and HCC (44). Intriguingly, our previous integrative epigenomics analysis has also revealed potential TGF $\beta$  and MAPK/JNK signal deregulation by EZH2 in HCC (29). In addition to  $\beta$ -catenin

signaling, whether functional cross-talk exists between HDAC8 and EZH2 in the epigenetic regulation of such pathways warrants further investigation.

SREBP-1 is a critical transcription factor linking lipid metabolism, insulin resistance, and cancer development (20–23). In accordance with a recent study that showed upregulation of SREBP-1 in human HCCs (45), we observed a significant correlation between SREBP-1 and HDAC8 in NAFLD-associated tumors from both murine models and clinical specimens. We further found that SREBP-1 directly upregulates HDAC8 through promoter occupancy, which in turn promotes insulin resistance *in vitro* and *in vivo*. Both gene knockdown and pharmacologic inhibition of HDAC8 in HCC cells significantly restore insulin sensitivity evident by enhanced insulin-stimulated AKT phosphorylation and lipogenic gene expressions (24, 46). Moreover, lentiviral-mediated *Hdac8* knockdown in the murine dietary obesity-NASH and -HCC models resulted in rectification of insulin sensitivity and restoration of normal metabolic profile. Although the molecular targets by which HDAC8 promotes insulin resistance remain to be defined, our findings underscore the importance of HDAC8 in aggravating metabolic deregulation during NAFLD-associated hepatocarcinogenesis.

Identification and selective targeting of the most critical cancer-specific chromatin regulators may reduce unspecific effects and increase antitumor efficacy, at least in part through subversion of cancer cell signaling (31). Accumulating preclinical and clinical studies have demonstrated the therapeutic efficacy of HDAC inhibition for the treatment of solid tumors (47). Drugging the histone methylome has also gained widespread interest because of the new findings of somatic mutations and mis-expression of histone methyltransferases such as EZH2 (48). Our present study delineates the molecular basis for the deregulation and oncogenicity of HDAC8 and EZH2 in NAFLD-associated hepatocarcinogenesis, which may aid deriving effective therapeutic strategies to tackle the alarming incidence of HCC amidst the obesity epidemic.

## Disclosure of Potential Conflicts of Interest

V.W.S. Wong has received speakers bureau honoraria from AbbVie, Echo-sens, Gilead, and Novartis and is a consultant/advisory board member for AbbVie, Gilead, Janssen, Novomedica, Otsuka, and Roche. G.L.H. Wong has received speakers bureau honoraria from AbbVie, Bristol-Myers Squibb, Echo-sens, Furui, Gilead, Janssen, and Otsuka and is a consultant/advisory board member for Gilead and Otsuka. H.L.Y. Chan has received speakers bureau honoraria from AbbVie, Bristol Myer Squibbs, Gilead, Novartis, and Roche and is a consultant/advisory board member for AbbVie, Abivax, Bristol Myer Squibbs, Gilead, Janssen, Novartis, and Roche. No potential conflicts of interest were disclosed by the other authors.

## Authors' Contributions

**Conception and design:** Y. Tian, V.W.S. Wong, G.L.H. Wong, T.H.M. Huang, K.F. To, A.S.L. Cheng, H.L.Y. Chan

**Development of methodology:** Y. Tian, G.L.H. Wong, J.H.M. Tong, M. Zhou, J. Yu, K.F. To

**Acquisition of data (provided animals, acquired and managed patients, provided facilities, etc.):** Y. Tian, W. Yang, J. Shen, J.H.M. Tong, Y.S. Cheung, M. Zhou, K.F. To

**Analysis and interpretation of data (e.g., statistical analysis, biostatistics, computational analysis):** Y. Tian, V.W.S. Wong, W. Yang, J. Shen, J.H.M. Tong, P.B.S. Lai, M. Zhou, K.F. To, A.S.L. Cheng, H.L.Y. Chan

**Writing, review, and/or revision of the manuscript:** Y. Tian, V.W.S. Wong, P.B.S. Lai, G. Xu, K.F. To, A.S.L. Cheng, H.L.Y. Chan



**Administrative, technical, or material support (i.e., reporting or organizing data, constructing databases):** H. Sun, J.H.M. Tong, M.Y.Y. Go, G. Xu, J. Yu, A.S.L. Cheng, H.L.Y. Chan

**Study supervision:** G.L.H. Wong, K.F. To, A.S.L. Cheng, H.L.Y. Chan

**Other (acquired funding support for this study):** A.S.L. Cheng

### Grant Support

This work was supported by the Theme-Based Research Scheme (T12-403/11), Collaborative Research Fund (C4017-14G), and the Hong Kong PhD

Fellowship Scheme of the Hong Kong Research Grants Council, National Natural Science Foundation of China (373492), and Focused Investment Scheme—Scheme B (1907301) of the Chinese University of Hong Kong.

The costs of publication of this article were defrayed in part by the payment of page charges. This article must therefore be hereby marked *advertisement* in accordance with 18 U.S.C. Section 1734 solely to indicate this fact.

Received December 23, 2014; revised August 1, 2015; accepted August 4, 2015; published OnlineFirst September 17, 2015.

### References

- Calle EE, Rodriguez C, Walker-Thurmond K, Thun MJ. Overweight, obesity, and mortality from cancer in a prospectively studied cohort of U.S. adults. *N Engl J Med* 2003;348:1625–38.
- Bhaskaran K, Douglas I, Forbes H, dos-Santos-Silva I, Leon DA, Smeeth L. Body-mass index and risk of 22 specific cancers: a population-based cohort study of 5.24 million UK adults. *Lancet* 2014;384:755–65.
- Altekruse SF, McGlynn KA, Reichman ME. Hepatocellular carcinoma incidence, mortality, and survival trends in the United States from 1975 to 2005. *J Clin Oncol* 2009;27:1485–91.
- Wong VW, Wong GL, Choi PC, Chan AW, Li MK, Chan HY, et al. Disease progression of non-alcoholic fatty liver disease: a prospective study with paired liver biopsies at 3 years. *Gut* 2010;59:969–74.
- Starley BQ, Calcagno CJ, Harrison SA. Nonalcoholic fatty liver disease and hepatocellular carcinoma: a weighty connection. *Hepatology* 2010;51:1820–32.
- Baffy C, Brunt EM, Caldwell SH. Hepatocellular carcinoma in non-alcoholic fatty liver disease: an emerging menace. *J Hepatol* 2012;56:1384–91.
- Ng M, Fleming T, Robinson M, Thomson B, Graetz N, Margono C, et al. Global, regional, and national prevalence of overweight and obesity in children and adults during 1980–2013: a systematic analysis for the Global Burden of Disease Study 2013. *Lancet* 2014;384:766–81.
- Zhang Z. Genomic landscape of liver cancer. *Nat Genet* 2012;44:1075–7.
- Totoki Y, Tatsuno K, Covington KR, Ueda H, Creighton CJ, Kato M, et al. Trans-ancestry mutational landscape of hepatocellular carcinoma genomes. *Nat Genet* 2014;46:1267–73.
- Kaelin WG Jr, McKnight SL. Influence of metabolism on epigenetics and disease. *Cell* 2013;153:56–69.
- Sassone-Corsi P. Physiology. When metabolism and epigenetics converge. *Science* 2013;339:148–50.
- Lu C, Thompson CB. Metabolic regulation of epigenetics. *Cell Metab* 2012;16:9–17.
- Murphy SK, Yang H, Moylan CA, Pang H, Dellinger A, Abdelmalek MF, et al. Relationship between methylome and transcriptome in patients with nonalcoholic fatty liver disease. *Gastroenterology* 2013;145:1076–87.
- Tian Y, Wong VW, Chan HL, Cheng AS. Epigenetic regulation of hepatocellular carcinoma in non-alcoholic fatty liver disease. *Semin Cancer Biol* 2013;23:471–82.
- Park EJ, Lee JH, Yu GY, He G, Ali SR, Holzer RG, et al. Dietary and genetic obesity promote liver inflammation and tumorigenesis by enhancing IL-6 and TNF expression. *Cell* 2010;140:197–208.
- Kohli R, Kirby M, Xanthakos SA, Softic S, Feldstein AE, Saxena V, et al. High-fructose, medium chain trans fat diet induces liver fibrosis and elevates plasma coenzyme Q9 in a novel murine model of obesity and nonalcoholic steatohepatitis. *Hepatology* 2010;52:934–44.
- Yu Z, Gao YQ, Feng H, Lee YY, Li MS, Tian Y, et al. Cell cycle-related kinase mediates viral-host signalling to promote hepatitis B virus-associated hepatocarcinogenesis. *Gut* 2014;63:1793–804.
- Feng H, Yu Z, Tian Y, Lee YY, Li MS, Go MY, et al. A CCRK-EZH2 epigenetic circuitry drives hepatocarcinogenesis and associates with tumor recurrence and poor survival of patients. *J Hepatol* 2015;62:1100–11.
- Feng H, Cheng AS, Tsang DP, Li MS, Go MY, Cheung YS, et al. Cell cycle-related kinase is a direct androgen receptor-regulated gene that drives beta-catenin/T cell factor-dependent hepatocarcinogenesis. *J Clin Invest* 2011;121:3159–75.
- Shao W, Espenshade PJ. Expanding roles for SREBP in metabolism. *Cell Metab* 2012;16:414–9.
- Moon YA, Liang C, Xie X, Frank-Kamenetsky M, Fitzgerald K, Kotliansky V, et al. The Scap/SREBP pathway is essential for developing diabetic fatty liver and carbohydrate-induced hypertriglyceridemia in animals. *Cell Metab* 2012;15:240–6.
- Jeon TI, Osborne TF. SREBPs: metabolic integrators in physiology and metabolism. *Trends Endocrinol Metab* 2012;23:65–72.
- Bakan I, Laplante M. Connecting mTORC1 signaling to SREBP-1 activation. *Curr Opin Lipidol* 2012;23:226–34.
- Shimomura I, Matsuda M, Hammer RE, Bashmakov Y, Brown MS, Goldstein JL. Decreased IRS-2 and increased SREBP-1c lead to mixed insulin resistance and sensitivity in livers of lipodystrophic and ob/ob mice. *Mol Cell* 2000;6:77–86.
- Balasubramanian S, Ramos J, Luo W, Sirisawad M, Verner E, Buggy JJ. A novel histone deacetylase 8 (HDAC8)-specific inhibitor PCI-34051 induces apoptosis in T-cell lymphomas. *Leukemia* 2008;22:1026–34.
- Li Y, Li X, Guo B. Chemopreventive agent 3,3'-diindolylmethane selectively induces proteasomal degradation of class I histone deacetylases. *Cancer Res* 2010;70:646–54.
- Vijayaraghavalu S, Dermawan JK, Cheriya V, Labhasetwar V. Highly synergistic effect of sequential treatment with epigenetic and anticancer drugs to overcome drug resistance in breast cancer cells is mediated via activation of p21 gene expression leading to G2/M cycle arrest. *Mol Pharm* 2013;10:337–52.
- Pez F, Lopez A, Kim M, Wands JR, Caron de Fromentel C, Merle P. Wnt signaling and hepatocarcinogenesis: molecular targets for the development of innovative anticancer drugs. *J Hepatol* 2013;59:1107–17.
- Cheng AS, Lau SS, Chen Y, Kondo Y, Li MS, Feng H, et al. EZH2-mediated concordant repression of Wnt antagonists promotes beta-catenin-dependent hepatocarcinogenesis. *Cancer Res* 2011;71:4028–39.
- You JS, Jones PA. Cancer genetics and epigenetics: two sides of the same coin? *Cancer Cell* 2012;22:9–20.
- Helin K, Dhanak D. Chromatin proteins and modifications as drug targets. *Nature* 2013;502:480–8.
- Buggy JJ, Sideris ML, Mak P, Lorimer DD, McIntosh B, Clark JM. Cloning and characterization of a novel human histone deacetylase, HDAC8. *Biochem J* 2000;350:199–205.
- Hu E, Chen Z, Fredrickson T, Zhu Y, Kirkpatrick R, Zhang GF, et al. Cloning and characterization of a novel human class I histone deacetylase that functions as a transcription repressor. *J Biol Chem* 2000;275:15254–64.
- Van den Wyngaert I, de Vries W, Kremer A, Neefs J, Verhasselt P, Luyten WH, et al. Cloning and characterization of human histone deacetylase 8. *FEBS Lett* 2000;478:77–83.
- Delcuve GP, Khan DH, Davie JR. Targeting class I histone deacetylases in cancer therapy. *Expert Opin Ther Targets* 2013;17:29–41.
- Waltregny D, De Leval L, Glenisson W, Ly Tran S, North BJ, Bellahcene A, et al. Expression of histone deacetylase 8, a class I histone deacetylase, is restricted to cells showing smooth muscle differentiation in normal human tissues. *Am J Pathol* 2004;165:553–64.
- Vannini A, Volpari C, Filocamo G, Casavola EC, Brunetti M, Renzoni D, et al. Crystal structure of a eukaryotic zinc-dependent histone deacetylase, human HDAC8, complexed with a hydroxamic acid inhibitor. *Proc Natl Acad Sci U S A* 2004;101:15064–9.
- Higuchi T, Nakayama T, Arai T, Nishio K, Yoshie O. SOX4 is a direct target gene of FRA-2 and induces expression of HDAC8 in adult T-cell leukemia/lymphoma. *Blood* 2013;121:3640–9.
- Wu J, Du C, Lv Z, Ding C, Cheng J, Xie H, et al. The up-regulation of histone deacetylase 8 promotes proliferation and inhibits apoptosis in hepatocellular carcinoma. *Dig Dis Sci* 2013;58:3545–53.
- Oehme I, Deubzer HE, Wegener D, Pickert D, Linke JP, Hero B, et al. Histone deacetylase 8 in neuroblastoma tumorigenesis. *Clin Cancer Res* 2009;15:91–9.

41. Mu S, Shimosawa T, Ogura S, Wang H, Uetake Y, Kawakami-Mori F, et al. Epigenetic modulation of the renal beta-adrenergic-WNK4 pathway in salt-sensitive hypertension. *Nat Med* 2011;17:573–80.
42. Kang Y, Nian H, Rajendran P, Kim E, Dashwood WM, Pinto JT, et al. HDAC8 and STAT3 repress BMF gene activity in colon cancer cells. *Cell Death Dis* 2014;5:e1476.
43. Yan W, Liu S, Xu E, Zhang J, Zhang Y, Chen X, et al. Histone deacetylase inhibitors suppress mutant p53 transcription via histone deacetylase 8. *Oncogene* 2013;32:599–609.
44. Seki E, Brenner DA, Karin M. A liver full of JNK: signaling in regulation of cell function and disease pathogenesis, and clinical approaches. *Gastroenterology* 2012;143:307–20.
45. Calvisi DF, Wang C, Ho C, Ladu S, Lee SA, Mattu S, et al. Increased lipogenesis, induced by AKT-mTORC1-RPS6 signaling, promotes development of human hepatocellular carcinoma. *Gastroenterology* 2011;140:1071–83.
46. Ide T, Shimano H, Yahagi N, Matsuzaka T, Nakakuki M, Yamamoto T, et al. SREBPs suppress IRS-2-mediated insulin signalling in the liver. *Nat Cell Biol* 2004;6:351–7.
47. West AC, Johnstone RW. New and emerging HDAC inhibitors for cancer treatment. *J Clin Invest* 2014;124:30–9.
48. McCabe MT, Ott HM, Ganji G, Korenchuk S, Thompson C, Van Aller GS, et al. EZH2 inhibition as a therapeutic strategy for lymphoma with EZH2-activating mutations. *Nature* 2012;492:108–12.